SIAM J. APPL. MATH.
Vol. 0, No. 0, pp. 000–000

SIR-NETWORK MODEL AND ITS APPLICATION TO DENGUE FEVER*

LUCAS M. STOLERMAN†, DANIEL COOMBS‡, AND STEFANELLA BOATTO§

Abstract. The SIR-network model, introduced in [S. Boatto et al., *SIR-Network Model for Epidemics Dynamics in a City*, in preparation] and [L. Stolerman, *Spreading of an Epidemic over a City: A Model on Networks*, Master's thesis, 2012 (in Portuguese)], deals with the propagation of disease epidemics in highly populated cities. The nodes, or vertices, are the city's neighborhoods, in which the local populations are assumed to be well-mixed. The directed edges represent the fractions of people moving from their neighborhoods of residence to those of daily activities. First, we present some fundamental properties of the basic reproduction number (R_o) for this model. In particular, we focus on how R_o depends upon the geometry and the heterogeneity (different infection rates in each vertex) of the network. This allows us to conclude whether an epidemic outbreak can be expected or not. Second, we submit the SIR-network model to data fitting, using data collected during the 2008 Rio de Janeiro dengue fever epidemic. Important conclusions are drawn from the fitted parameters, and we show that improved results are found when a time-dependent infection parameter is introduced.

Key words. metapopulation models, stability analysis, complex networks, dengue epidemics, data fitting

AMS subject classifications. 92D30, 34D20, 92B05, 92C42

DOI. 10.1137/140996148

1. Introduction.

Dengue fever is an infectious viral disease occurring in humans that is prevalent in parts of Central and South America, Africa, India, and Southeast Asia. Recent estimates indicate that several hundred million new infections occur per year worldwide [4]. Although the majority of infections are believed to be mild or asymptomatic, a small fraction of infected individuals develop serious hemorrhagic fever, and there is currently no effective antiviral therapy or vaccination available beyond the trial stage [31]. The main disease vector is the *Aedes aegypti* mosquito, even though a second mosquito, *Aedes albopictus*, is shown to play a nonnegligible role in the spread of dengue in more rural areas, as reported by the U.S. Centers for Disease Control and Prevention [7, 20] and evidenced by the recent appearance of some autochthonous cases of dengue in southern France [15]. The *Aedes aegypti* mosquito is believed to be primarily human-biting, and it is well adapted to life in

*Received by the editors November 17, 2014; accepted for publication (in revised form) August 27, 2015; published electronically DATE.
http://www.siam.org/journals/siap/x-x/99614.html

†Posgraduação Instituto de Matemática, Universidade Federal de Rio de Janeiro, Rio de Janeiro, RJ 21941-901, Brazil, and Instituto Nacional de Matemática Pura e Aplicada (IMPA), Estrada Dona Castorina 110, Rio de Janeiro, RJ 22460-320, Brazil (Lucasms@impa.br). This author's work was supported by an Emerging Leaders in the Americas scholarship from the Canadian Department of Foreign Affairs, Trade and Development, and by CAPES (Coordenação de Aperfeiçoamento de Pessoal de Nível Superior).

‡Department of Mathematics and Institute of Applied Mathematics, University of British Columbia, 1984 Mathematics Road, Vancouver, BC V6T 1Z2, Canada (coombs@math.ubc.ca). This author's work was supported by the Natural Science and Engineering Research Council of Canada.

§Departamento de Matemática Aplicada, Instituto de Matemática, Universidade Federal de Rio de Janeiro, Av. Athos da Silveira Ramos 149, Edificio do Centro de Tecnologia, Bloco C Caixa Postal 68530, Ilha do Fundão, CEP 21941-909, Rio de Janeiro, RJ, Brazil (boatto.stefanella@gmail.com). This author's work was supported by CAPES and FAPERJ (Fundação Carlos Chagas Filho de Amparo à Pesquisa do Estado do Rio de Janeiro).

urban and semi-urban environments, where it lays its eggs in natural and artificial water containers. Its lifetime movement range has been found to be typically less than a kilometer [17, 8], and therefore the spread of dengue through an urban area is most likely driven by everyday human movement: in effect, humans are acting as vectors between relatively localized mosquito populations [1].

In this context, the SIR-network model, introduced in [5, 32], is a rather interesting simplified model since it captures the impact of human mobility on the occurrence of an epidemic outbreak. In particular, in adapting this model as a simplification of the dengue fever dynamics, the local infection parameters express environmental properties such as the mosquito population and variations in human behavior across neighborhoods. We want to stress that in our model we do not deal explicitly with the mosquito infection dynamics as, for example, in [24]. Also, we do not take into consideration the incubation period of dengue fever in humans or mosquitoes. Rather, we will focus on the importance of human mobility and the geometry/heterogeneity of the network on the occurrence of an epidemic outbreak. In what follows, we stress the lack of robustness of homogeneous networks, namely, those whose vertices have all the same values of the infection parameter. More specifically, in a homogeneous network the mobility of people is irrelevant, while in a slightly heterogeneous network it could be an essential ingredient in avoiding an epidemic.

The paper is organized as follows. In section 2 we briefly introduce the SIR-network model. For a comprehensive discussion about the formulation of the model, see [5]. In section 3 we show the link between the basic reproduction number R_o and stability analysis of the nonlinear system of ODEs of the SIR-network model. We then derive a method for evaluating R_o in a general framework. In section 4 we address the following question: *Under which conditions does an epidemic outbreak occur?* We make use of the R_o criterion to determine when an epidemic would occur: an infected individual, introduced in a disease-free population, would generate more than one secondary infection on average; see Figure 1(a). In section 5 we show that our numerical simulations are in agreement with the theorems introduced in section 4. The second part of this work begins in section 6, where some data fitting is done with the SIR-network model. Choosing a special region of the city of Rio de Janeiro, we estimate the values of the epidemiological parameters and obtain some interesting conclusions. Better fits are obtained in section 7, where we introduce a Gaussian-like time varying infection parameter, in order to model climate changes (in particular, the influence of seasonal climate changes) during one year in the city.

2. The SIR-network model.

2.1. A city as a network of neighborhoods: A metapopulation model. Metapopulation models are commonly used to describe the dynamics of an epidemic in a heterogeneous environment [2, 3, 16, 21, 26]. For example, Arino and van den Driessche studied the spread of a disease between different cities, considering the possibility of migration between them [2]. Their results showed the importance of human mobility in the problem of the occurrence of an epidemic. However, in the case of dengue in a single urban area, we are more interested in everyday movement between neighborhoods, as previously modeled by Adams and Kapan [1]. For this reason the smallest time scale in our model is a day, and thus we can neglect the slower dynamics of migration and demography.

It is interesting to think about the structure of the metapopulation network. At one extreme, we could work at the small scale, where each patch is roughly the size of a single metapopulation of mosquitoes. Since each mosquito can travel at most

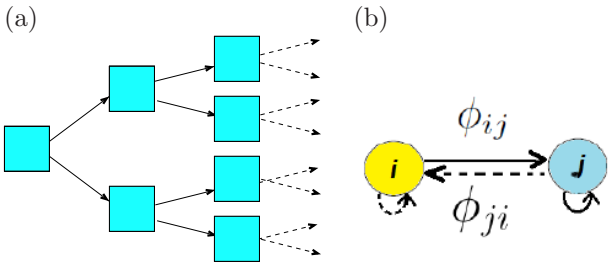

FIG. 1. (a) *The basic reproduction number $R_o = 2$: An infected individual, introduced in a disease-free population, would generate two secondary infection on average;* (b) *ϕ_{ij}: Fraction of people moving daily from the neighborhood i to the neighborhood j.*

only a few hundred meters, this means that we would consider each patch as just a few city blocks or a single apartment complex. On the other hand, we could also imagine dividing a large city coarsely into regions with populations of many hundreds of thousands of people. The choice of this scale should be driven by the available detailed data on mosquito abundances and human travel patterns within the city. Another interesting point to investigate is the influence of the geometry of the human transport network on the spread of the disease. This can be measured using data from road traffic studies and public transportation companies. For huge cities such as Rio de Janeiro, it is usual to find that some regions have stronger connections than others. Finally, there is the ecological *heterogeneity* of the network patches from the point of view of mosquito populations. In the case of dengue fever transmitted by *Aedes aegypti*, we would expect a strong correlation between collections of standing water near houses and the transmission rate of the virus.

Mathematically, we assume that the city has M neighborhoods (corresponding to vertices of the network) and we denote this set as $V = \{1, 2, \ldots, M\}$. A vertex i is linked to another j if there is a fraction of residents of i that travel to j and back daily. Graphically, we shall denote this with an arrow going from the node i to the node j, as shown in Figure 1(b). Note that the edges are not bidirectional, since there may generally be residential networks that are not significant employment centers. In this case the network is said to be asymmetric. The *geometry* of the network is then defined by specifying the *flux matrix* $\mathbf{\Phi}$,

$$\mathbf{\Phi}_{M\times M} = \begin{pmatrix} \phi_{11} & \phi_{12} & \cdots & \phi_{1M} \\ \phi_{21} & \phi_{22} & \cdots & \phi_{2M} \\ \vdots & \vdots & \ddots & \vdots \\ \phi_{M1} & \phi_{M2} & \cdots & \phi_{MM} \end{pmatrix}, \tag{2.1}$$

whose entries $\phi_{ij} \in [0, 1]$ are the fraction of resident population going from i to j. It is important to note that the ϕ_{ij}'s are dimensionless. As discussed in more detail in [5], we assume that there is conservation of the resident population at each node, and therefore we require that the fractions satisfy

$$\sum_{k=1}^{M} \phi_{ik} = 1 \quad \forall i \in V. \tag{2.2}$$

2.2. The equations. As the name *network model* suggests, our equations are inspired by those of the basic one-compartment SIR model. The system

$$\dot{S} = -\beta S(t)\frac{I(t)}{N}, \tag{2.3}$$

$$\dot{I} = \beta S(t)\frac{I(t)}{N} - \gamma I(t), \tag{2.4}$$

$$\dot{R} = \gamma I(t) \tag{2.5}$$

is well known in the field and was first presented by Kermack and McKendrick in their now famous paper [22]. The variables $S(t)$, $I(t)$, and $R(t)$ are, respectively, the numbers of susceptible, infected, and recovered individuals of a constant size population. The SIR model ignores almost every detail of a real epidemic except for transmission, which is assumed to occur as a mass-action effect—the population is well-mixed in regard to age, social structure, etc., with respect to transmission (reviewed in [36, 12, 32]). These equations are a special case of the more complex and general model originally proposed by Kermack and McKendrick [22] that included epidemiological parameters depending on the time since infection, leading to a system of integro-differential equations.

We set up the SIR-network system as follows. Suppose that people in each neighborhood are either susceptible, infected, or removed. In the interest of simplicity, we ignore both the transient noninfectious period following a new infection and the potential for re-infection by another strain of dengue. We also ignore the dynamics of infection of mosquitoes within each patch and simply assume that the per-time probability of transmission between humans is fixed. This is equivalent to assuming that the proportion of infectious mosquitoes in a patch is proportional to the proportion of infected humans in that patch.

For any vertex $i \in V$, let $S_i(t)$, $I_i(t)$, and $R_i(t)$ be the number of susceptible, infected, and removed individuals, respectively, in neighborhood i at time t. The total population *resident* at i is assumed to be constant in time and is given by

$$N_i = S_i(t) + I_i(t) + R_i(t).$$

Moreover, since $\phi_{ki}N_k$ is the total population at vertex k that travels every day to vertex i, it will be necessary to define

$$N_i^p = \sum_{k=1}^{M} \phi_{ki}N_k$$

as the *present* population at i, which is also constant in time. Following Arino and van den Driessche [2], N_i^p will be a normalizing factor for the equations.

For the epidemiological parameters, we set β_j as the infection rate at patch j for all $j \in V$. This is a lumped parameter that is determined by the density of mosquitoes in the jth patch, their biting rate, and the probability of transmission by human to and from the vector. We set the recovery/removal rate for infected individuals to be γ and assume that this is constant across all patches of the network. The dynamics of $S_i(t)$, $I_i(t)$, and $R_i(t)$ are then modeled by the following first-order homogeneous

system of differential equations:

$$\dot{S}_i(t) = -\sum_{j=1}^{M}\sum_{k=1}^{M} \beta_j \phi_{ij} S_i \frac{\phi_{kj} I_k}{N_j^p}, \tag{2.6}$$

$$\dot{I}_i(t) = \sum_{j=1}^{M}\sum_{k=1}^{M} \beta_j \phi_{ij} S_i \frac{\phi_{kj} I_k}{N_j^p} - \gamma I_i, \tag{2.7}$$

$$\dot{R}_i(t) = \gamma I_i. \tag{2.8}$$

The double-summation term allows for infection of any resident of patch i, at location j, by an individual from patch k, provided the relevant elements of ϕ_{ij} are nonzero.

3. The basic reproduction number R_o for the SIR-network model. In epidemiology, a very fundamental problem is to estimate how many new infections are caused by a single infected individual, over the course of their infection, at the start of the epidemic. This number is called the basic reproduction number and is denoted by R_o. In a big enough population, an epidemic outbreak will take place if and only if $R_o > 1$. This threshold property has a biological inspiration, and the mathematical theory of R_o is well described in [12, 13, 14, 18].

In order to establish R_o for the SIR-network model, we begin by introducing the vector notation, since the infected individuals are from different vertices of the network. Let $S_i^* = N_i$ and $I_i^* = 0$ be, respectively, the equilibrium population of the healthy and infected populations at the node i. At instant t we define

$$\mathbf{S}(t) = (S_1(t), S_2(t), \ldots, S_M(t))^T, \qquad \Delta\mathbf{S}(t) = (\Delta S_1(t), \Delta S_2(t), \ldots, \Delta S_M(t))^T,$$

$$\mathbf{I}(t) = (I_1(t), I_2(t), \ldots, I_M(t))^T, \qquad \Delta\mathbf{I}(t) = (\Delta I_1(t), \Delta I_2(t), \ldots, \Delta I_M(t))^T,$$

where $S_i(t) = S_i^* + \Delta S_i(t)$ and $I_i(t) = I_i^* + \Delta I_i(t)$ $(i = 1, \ldots, M)$ represent, respectively, the number of healthy and infected individuals at the node i at the time t. Substituting the perturbation forms into (2.6) and linearizing, we obtain

$$\frac{d\Delta\mathbf{I}}{dt}(t) = (\mathbf{B} - \gamma\mathbb{I})\Delta\mathbf{I}(t) = \gamma(\mathcal{K} - \mathbb{I})\Delta\mathbf{I}(t).$$

The corresponding discrete equations are

$$\Delta\mathbf{I}(t_{n+1}) = [\mathbb{I} + \gamma\,\Delta t\,(\mathcal{K} - \mathbb{I})\Delta\mathbf{I}(t_n)], \tag{3.1}$$

where

(3.2)

$$\mathcal{K} = \frac{1}{\gamma}\mathbf{B},$$

$$= \frac{1}{\gamma}\begin{pmatrix} \sum_{j=1}^{M}\beta_j\phi_{1j}\phi_{1j}\frac{N_1}{N_j^p} & \sum_{j=1}^{M}\beta_j\phi_{1j}\phi_{2j}\frac{N_1}{N_j^p} & \cdots & \sum_{j=1}^{M}\beta_j\phi_{1j}\phi_{Mj}\frac{N_1}{N_j^p} \\ \sum_{j=1}^{M}\beta_j\phi_{2j}\phi_{1j}\frac{N_2}{N_j^p} & \sum_{j=1}^{M}\beta_j\phi_{2j}\phi_{2j}\frac{N_2}{N_j^p} & \cdots & \sum_{j=1}^{M}\beta_j\phi_{2j}\phi_{Mj}\frac{N_2}{N_j^p} \\ \vdots & \vdots & \ddots & \vdots \\ \sum_{j=1}^{M}\beta_j\phi_{Mj}\phi_{1j}\frac{N_M}{N_j^p} & \sum_{j=1}^{M}\beta_j\phi_{Mj}\phi_{2j}\frac{N_M}{N_j^p} & \cdots & \sum_{j=1}^{M}\beta_j\phi_{Mj}\phi_{Mj}\frac{N_M}{N_j^p} \end{pmatrix}$$

is the well-known *next generation matrix* (NGM); see [13, 18] for references. Notice that if the time step is chosen to be $\Delta t = \frac{1}{\gamma}$, (3.1) reduces to

$$\Delta \mathbf{I}(t_{n+1}) = \mathcal{K} \Delta \mathbf{I}(t_n). \tag{3.3}$$

Notation. Since the equilibrium state $\mathrm{I}_j^* = 0$, for all $j = 1, \dots, M$, from now on we shall identify $\mathbf{I}(t_n) = \Delta \mathbf{I}(t_n)$. We summarize this in the following.

PROPOSITION 1. *Let $(V, \Phi_{M\times M})$ be the network given by a vertices set $V = \{1, 2, \dots, M\}$ and a flux matrix $\Phi = [\phi_{ij}]_{M\times M}$ of the system (2.6), describing the SIR-network dynamics. Then, by considering $\Delta t = \frac{1}{\gamma}$ and $\mathcal{K}$ as in (3.3), we have that*

$$\boldsymbol{I}(t_{n+1}) = \mathcal{K} \boldsymbol{I}(t_n)$$

describes the discrete dynamics of the system linearized about the equilibrium state $(S_i^*, I_i^*) = (N_i, 0)$ for all $i \in V$. In particular, the first generation of infected individuals is given by

$$\boldsymbol{I}(t_1) = \mathcal{K} \boldsymbol{I}_0.$$

Remark. The NGM $\mathcal{K}$ is an $M \times M$ matrix, where

$$\mathcal{K}(i,k) = \frac{1}{\gamma} \sum_{j=1}^{M} \beta_j \phi_{ij} \phi_{kj} \frac{N_i}{N_j^p}$$

for all $(i, k) \in V \times V$. For a fixed j, the term

$$\frac{\beta_j}{\gamma} \phi_{ij} \phi_{kj} \frac{N_i}{N_j^p}$$

represents the average number of infected individuals residing at the vertex i which were infected at a node j by an infected individual residing at the node k. Here we can see a correspondence with the expression for the basic reproduction number for the SIR model (2.3), which is given by $R_o = \frac{\beta}{\gamma}$. Therefore, the sum $\mathcal{K}(i, k)$ represents the average number of infected individuals residing in vertex i which were infected by a single infected individual introduced at vertex k.

Following the result of Proposition 1, if we introduce an infected individual in a disease-free population through neighborhood i, i.e., if $I_i(0) = 1$ for some $i \in V$ and $I_j(0) = 0$ otherwise, then the sum

$$\sum_{k=1}^{M} \mathcal{K}(k, i)$$

could be a good definition for R_o. However, it depends on the vertex i, so it may vary from one vertex to another. Hence, we follow previous work [13, 18] and state the following definition.

DEFINITION. *Given the NGM $\mathcal{K}$, (3.3), the basic reproduction number is defined to be*

$$R_o = \lim_{n\to\infty} ||\mathcal{K}^n||^{\frac{1}{n}}, \tag{3.4}$$

where $||\mathcal{K}^n|| = \sup_{||u||=1} ||\mathcal{K}^n u||$ and $||u|| = \sum_{i=1}^{M} u_i$.

Remarks. (a) Notice that, in the asymptotic limit of an infinite number of generations, the *basic reproduction number* R_o, defined above, is an average of the *per-generation* factor (see [32, 13, 18] for a detailed discussion of this definition).

(b) The expression of (3.4) is the definition of the spectral radius of the matrix $\mathcal{K}$. It can be shown that, for an *irreducible*[1] matrix $\mathcal{K}$, it coincides with the largest eigenvalue of $\mathcal{K}$ (for references on matrix analysis, see [19, 25]). In fact, once $\mathcal{K} \geq 0$ (i.e., $\mathcal{K}(i,j) \geq 0$ for all $(i,j) \in V \times V$), the Perron–Frobenius theory guarantees that if $\mathcal{K}$ is irreducible, then R_o is the largest real positive eigenvalue of $\mathcal{K}$. Furthermore, since the equilibrium solution $((S_i^*, I_i^*) = (N_i, 0)$ for all $i \in V)$ is unstable for $R_o > 1$, the definition (3.4) preserves the threshold property and hence the biological meaning of R_o.

4. Analytical estimates. Let's now go back to our network with M vertices (neighborhoods) and a flux matrix $\Phi_{M\times M}$, (2.1), outlined in section 3. We denote such a network by $(V, \Phi_{M\times M})$, where $V = \{1, 2, \ldots, M\}$ is the set of all vertices. We model the epidemic dynamics by the set of equations (2.6) which, in general, depend on the vertex-dependent parameters β_j and N_j, which are, respectively, the infection rate and the resident population at vertex j, on the vertex-independent recovery rate γ, and on Φ_{jk}, which describe how people resident in neighborhood j travel to and from neighborhood k. The following questions naturally arise:

1. *Under which conditions does an epidemic occur*?
2. *When it occurs, how does it spread through the city (i.e., the network)*?

Following what was outlined in section 3, we address the first question by seeking an explicit expression for basic reproduction number R_o, which, as seen in the previous section, coincides with the maximum eigenvalue of the next generation matrix $\mathcal{K}$, (3.3). From the mathematical point of view, investigating whether R_o is greater than 1 (or not) is the same as establishing the local stability of the disease-free equilibrium point. Once we have computed R_o, we make use of the following criterion.

R_o criterion.[2] If the NGM is irreducible, then epidemics occur if and only if $R_o > 1$.

All this seems rather simple and straightforward; however, for our model, to analyze R_o might not be such a trivial task, as it depends upon a large number of parameters: $M^2 + 2M + 1$ parameters for a network of M nodes. A general theory encompassing all possible network models will be difficult to develop. Therefore, we will present results for a small class of network models with carefully defined within- and between-neighborhood properties.

DEFINITION. *We define a homogeneous network model to be one where all the nodes have the same rate of infection, $\beta_j = \beta_o$ for all $j = 1, \ldots, M$. All other network models are defined to be heterogeneous.*

Making this definition allows us to distinguish the roles played by network geometry and movement parameters. In what follows, we will also be able to study

[1] From MathWorld (http://mathworld.wolfram.com/ReducibleMatrix.html): A matrix is reducible if and only if it can be placed into block upper-triangular form by simultaneous row/column permutations. In addition, a matrix is reducible if and only if its associated digraph is not strongly connected. A square matrix that is not reducible is said to be *irreducible*.

See also the definitions in section 6.2.21 of Horn and Johnson [19]. An equivalent definition is the following from [12].

DEFINITION. *A nonnegative matrix $\mathcal{K}$ is called* irreducible *if for every index pair i, j there exists an integer $m = m(i,j) > 0$ such that $\mathcal{K}^m(i,j) > 0$.*

[2] As further investigated in [35], when the parameters β_j are time dependent, this is necessary but not sufficient to deduce the occurrence of an epidemic.

the robustness of results for homogeneous network models when an inhomogeneity is introduced, such as, for example, a different infection rate in one of the nodes as in the example given in Figure 2. From an epidemiological point of view, this distinction is also important in terms of modeling vector-driven epidemics (such as dengue) versus epidemics driven by direct human-to-human contact. In the former case, we can easily imagine variations in transmissibility due to variations in mosquito density. However, in the latter case, local variations in human behavior might be neglected, leading to a homogeneous network model with respect to the rates of infection.

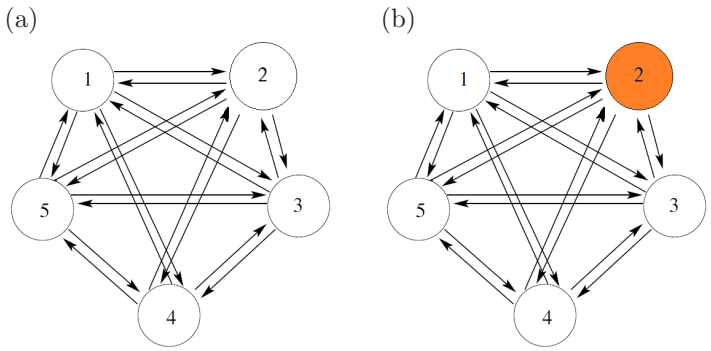

FIG. 2. (a) *Homogeneous fully connected $N =$ network: All nodes have the same infection rate β_o.* (b) *Heterogeneous fully connected network with a node with a different infection rate: $\beta_j = \beta_o$ for $j \neq 2$ and $\beta_2 \neq \beta_o$.*

4.1. Homogeneous network models. The following theorem shows that when all the vertices have the same infection rate β_o, the basic reproductive number, which we call R_o^{hom} in this case, is simply equal to β_o/γ. Therefore, irrespective of the movements of the population, an epidemic occurs if and only if $\beta_o > \gamma$. This is consistent with the fact that if $\beta_o > \gamma$, an epidemic could occur independently in any neighborhood. Conversely, if the conditions for an epidemic do not exist in any neighborhood, then no epidemic is possible.

THEOREM 1. *Let $(V, \Phi_{M\times M})$ be a network associated to the SIR-network system (2.6). Let $\beta_o > 0$ be a constant value such that*

$$\beta_j = \beta_o \quad \forall j \in V.$$

Then we have $R_o^{hom} = \frac{\beta_o}{\gamma}$, and hence epidemics are possible if and only if $\beta_o > \gamma$.

Remark. Theorem 1 remains valid even when the associated NGM is reducible. So this result is about networks of general geometry—even disconnected networks. In this particular case, the epidemic only occurs inside the connected part(s), where the infection has been introduced.

The proof of this theorem relies on the fact that, in this special case, the NGM is given by

$$\mathcal{K} = \frac{\beta_0}{\gamma}\mathcal{C},$$

where

$$\mathcal{C} = \begin{pmatrix} \sum_{j=1}^{M} \phi_{1j}\phi_{1j}\frac{N_1}{N_j^p} & \sum_{j=1}^{M} \phi_{1j}\phi_{2j}\frac{N_1}{N_j^p} & \cdots & \sum_{j=1}^{M} \phi_{1j}\phi_{Mj}\frac{N_1}{N_j^p} \\ \sum_{j=1}^{M} \phi_{2j}\phi_{1j}\frac{N_2}{N_j^p} & \sum_{j=1}^{M} \phi_{2j}\phi_{2j}\frac{N_2}{N_j^p} & \cdots & \sum_{j=1}^{M} \phi_{2j}\phi_{Mj}\frac{N_2}{N_j^p} \\ \vdots & \vdots & \ddots & \vdots \\ \sum_{j=1}^{M} \phi_{Mj}\phi_{1j}\frac{N_M}{N_j^p} & \sum_{j=1}^{M} \phi_{Mj}\phi_{2j}\frac{N_M}{N_j^p} & \cdots & \sum_{j=1}^{M} \phi_{Mj}\phi_{Mj}\frac{N_M}{N_j^p} \end{pmatrix}.$$

The following lemma is used to show that $\lambda = 1$ is an eigenvalue of $\mathcal{C}$.

LEMMA 1. *The matrix $\mathcal{C}$ defined above has $v = \frac{1}{N_M}(N_1, N_2, \ldots, N_M)^T$ as an eigenvector with corresponding eigenvalue $\lambda = 1$.*

Proof of the lemma. Let's consider $\mathcal{C}$, as defined in (4.1), and $v = (\frac{N_1}{N_M}, \frac{N_2}{N_M}, \ldots, \frac{N_M}{N_M})^T$. Then the product matrix $\mathcal{C}v$ is

$$\mathcal{C}v = \begin{pmatrix} \sum_{j=1}^{M} \phi_{1j}\phi_{1j}\frac{N_1}{N_j^p} & \sum_{j=1}^{M} \phi_{1j}\phi_{2j}\frac{N_1}{N_j^p} & \cdots & \sum_{j=1}^{M} \phi_{1j}\phi_{Mj}\frac{N_1}{N_j^p} \\ \sum_{j=1}^{M} \phi_{2j}\phi_{1j}\frac{N_2}{N_j^p} & \sum_{j=1}^{M} \phi_{2j}\phi_{2j}\frac{N_2}{N_j^p} & \cdots & \sum_{j=1}^{M} \phi_{2j}\phi_{Mj}\frac{N_2}{N_j^p} \\ \vdots & \vdots & \ddots & \vdots \\ \sum_{j=1}^{M} \phi_{Mj}\phi_{1j}\frac{N_M}{N_j^p} & \sum_{j=1}^{M} \phi_{Mj}\phi_{2j}\frac{N_M}{N_j^p} & \cdots & \sum_{j=1}^{M} \phi_{Mj}\phi_{Mj}\frac{N_M}{N_j^p} \end{pmatrix} \begin{pmatrix} \frac{N_1}{N_M} \\ \frac{N_2}{N_M} \\ \vdots \\ \frac{N_M}{N_M} \end{pmatrix}.$$

Observe that the i*th* row is

$$\begin{aligned} (\mathcal{C}v)_i &= \sum_{l=1}^{M} \mathcal{C}_{il}\frac{N_l}{N_M} = \sum_{l=1}^{M}\left(\sum_{j=1}^{M}\frac{\phi_{ij}\phi_{lj}N_i}{N_j^p}\right)\frac{N_l}{N_M} \\ &= \frac{N_i}{N_M}\sum_{j=1}^{M}\sum_{l=1}^{M}\frac{\phi_{ij}N_l\phi_{lj}}{\sum_{k=1}^{M}N_k\phi_{kj}} = \frac{N_i}{N_M}\sum_{j=1}^{M}\phi_{ij}\frac{\sum_{l=1}^{M}N_l\phi_{lj}}{\sum k = 1^M N_k\phi_{kj}} \\ &= \frac{N_i}{N_M}\sum_{j=1}^{M}\phi_{ij} = \frac{N_i}{N_M} = v_i, \end{aligned}$$

where we have made use of the conservation law $\sum_{j=1}^{M}\phi_{ij} = 1$. Therefore, $\mathcal{C}v = v$, and v is an eigenvector of $\mathcal{C}$ with corresponding eigenvalue $\lambda = 1$. ∎

The proof of Theorem 1 follows immediately, since the standard Perron–Frobenius theory (see, e.g., Corollary 8.1.30 in [19]) allows us to conclude that $\lambda = 1$ is indeed the spectral radius of $\mathcal{C}$. Therefore, $R_o^{\text{hom}} = \beta_0/\gamma$, as stated in Theorem 1.

4.2. Heterogeneous fully connected network models. Starting from a homogeneous network model, let's introduce an inhomogeneity in one of the nodes. The crucial question is whether this perturbation can qualitatively change the analysis of the previous section; in other words, we are testing the robustness of a homogeneous network. In this section, we illustrate this concept with an example. We consider a *fully connected network*, and we just choose to have a different value of the infectivity parameter at one of the nodes, chosen without loss of generality as the second node:

$$\beta_2 = \beta_o\zeta \qquad \text{and} \qquad \beta_k = \beta_o, \qquad k = 1, 3, 4, \ldots, M, \tag{4.1}$$

where M is the number of nodes. The multiplicative factor ζ modifies the infectivity at the second node. We remind the reader that a fully connected network is a network

in which each node is connected to every other node. We further assume that the fractions of movement between any two nodes is a constant $\phi_o > 0$. We can then use the conservation law, (2.2), to parametrize the entries of the flux matrix ($\Phi_{M\times M}$), (2.1), as

$$\phi_{ij} = \begin{cases} \phi_o & \text{if} \quad i \neq j, \\ 1-(M-1)\phi_o & \text{if} \quad i = j, \end{cases} \tag{4.2}$$

where $0 < \phi_o \leq \frac{1}{M-1}$, so the flux matrix Φ has nonnegative entries.

THEOREM 2. *Let $V = \{1, 2, 3, \ldots, M\}$, and let $\Phi_{M\times M}$ be defined by* (4.2). *We suppose that the populations at the nodes are equal, $N_i = N_o > 0$ for all $i \in V$, and that* (4.1) *holds. Under these conditions, we can calculate the basic reproductive number for the heterogeneous system and obtain conditions guaranteeing the stability of the disease-free equilibrium. More precisely, if we consider the case where the background nodes are stable, that is, $R_o^{hom} = \beta_0/\gamma < 1$, there is a minimum value of ζ that leads to guaranteed instability of the whole system, given by*

$$\zeta^{crit} = 1 + \frac{(1 - R_o^{hom})}{R_o^{hom}} M. \tag{4.3}$$

In the case $1/R_o^{hom} < \zeta < \zeta^{crit}$, there is an interval

$$\mathcal{I} = \left(\max\left\{0, \frac{1}{M} - \tilde{\phi}\right\}, \min\left\{\frac{1}{M-1}, \frac{1}{M} + \tilde{\phi}\right\}\right),$$

where

$$\tilde{\phi} = \frac{1}{M}\sqrt{\frac{M(1-R_o) - R_o(\zeta - 1)}{R_o\left(M\zeta(1-R_o) - (\zeta-1)\right)}}$$

such that if $\phi_o \in \mathcal{I}$, the disease-free equilibrium is stable, and otherwise it is unstable. Finally, when $\zeta < 1/R_o^{hom}$, the disease-free equilibrium is always stable.

Numerical simulations are in agreement with the theorem above, as shown in section 5.2. A proof of this theorem can be found in the appendix.

Remark. Theorem 2 shows a quite important property of vector based epidemics. When vectors (in many cases, mosquitoes) are present, it is evident that a network will not generally be *homogeneous* since, in this case, the β_i parameters represent not only the population densities of mosquitoes—which could vary depending on the local topography and vegetation—but also the way humans are protecting themselves from contact with the mosquitoes and possibly controlling the mosquito population. In the case of dengue fever in a large city like Rio de Janeiro, this is connected to the fact that the human population network is highly heterogeneous. Theorem 2 shows how in this case epidemics could be avoided by dilution (*flux*) of the number of infected individuals, from the neighborhoods with high infectivity parameter β to the neighborhoods with low β. In other words, the control of vector-borne epidemics could be quite different from that of epidemics driven by direct contact.

5. Numerical simulations.

5.1. Homogeneous networks. We now present some examples to illustrate the theory described above. In Figure 3, we show results from numerical integration of the system of (2.6) for a fully connected network with five nodes ($M = 5$). We

have chosen a population of $N_j = 10^4$ individuals at each node and set the recovery time scale to one week by choosing $\gamma = 1/\text{week}$. The initial conditions are always chosen such that we have a single infected individual in node one and the rest of the population is completely susceptible:

$$S_1(0) = N_0 - 1,\ I_1(0) = 1,\ R_1(0) = 0,\ S_2(0) = N_0,\ I_2(0) = 0,\ R_2(0) = 0.$$

The transmissibility coefficients β_i are chosen as above so that $\beta_1 = \zeta\beta_o$ and $\beta_j = \beta_o$ for $j = 2, 3, 4, 5$. In Figure 3, we choose $\beta_o = 0.7$ and $\zeta = 4$. This means that in the absence of mixing, an epidemic could only occur in node 1. Results are shown for low, medium, and high values of the parameter ϕ_o. We can observe that, although epidemics occur for all fractions ϕ_o, the relative sizes of the epidemics in node 1 and the other nodes depend strongly on the extent of population mixing. The timing and magnitude of the epidemics also vary since the basic reproductive number depends on ϕ_o.

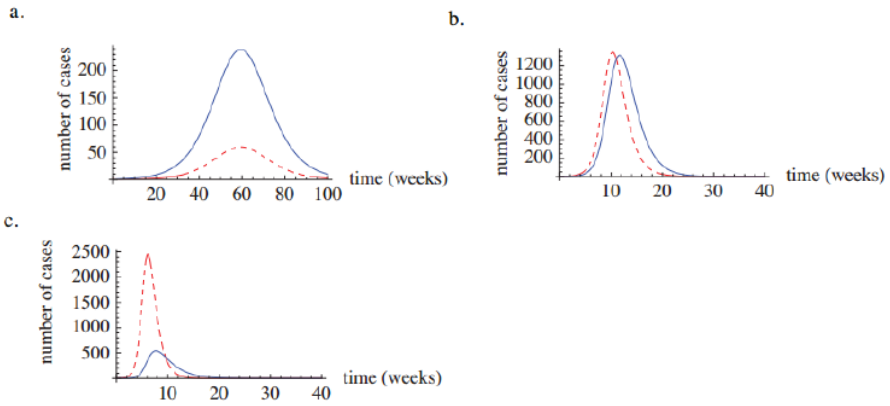

FIG. 3. *Epidemic time courses are plotted for low, medium, and high values of the population mixing parameter, $\phi_o = 0.01, 0.05, 0.1$, respectively. Numbers of infected individuals are shown for node 1 alone (dotted lines) and the sum of nodes 2–5 (solid lines). Parameter values are given in the text.*

Next, we verify the application of Theorem 2 by plotting the peak number of infected people over the course of an epidemic, while varying ζ and ϕ_o. This is done to numerically verify that for certain values of the infectivity multiplier ζ, there exists an interval $\mathcal{I}$ such that if $\phi_o \in \mathcal{I}$, no epidemic can occur.

In Figure 4 we show the results of our simulations for three different scenarios corresponding to different background infectiousnesses β_o. In each case, we use $M = 5$ nodes and set $\gamma = 1/\text{week}$. Figure 4(a) shows plots of the peak size of the epidemic (summed across all nodes) as a function of ϕ_o, for a range of possible ζ leading to epidemics. In this case the background infectiousness is $\beta_o = 0.5$, and hence $\zeta^{\text{crit}} = 6$. For all values of ζ exceeding ζ^{crit}, an epidemic occurs. We can observe (Figure 4(d)) that for $\zeta = 5.75$, there is a range of ϕ_o where no epidemic occurs. This is in agreement with Theorem 2, which indicates that when $\zeta = 5.75$, no epidemic occurs for $\phi_o \in \mathcal{I} = (0.168, 0.232)$. Panels (b) and (c) of Figure 4 show results for $\beta_o = 0.7$ and 0.9, respectively.

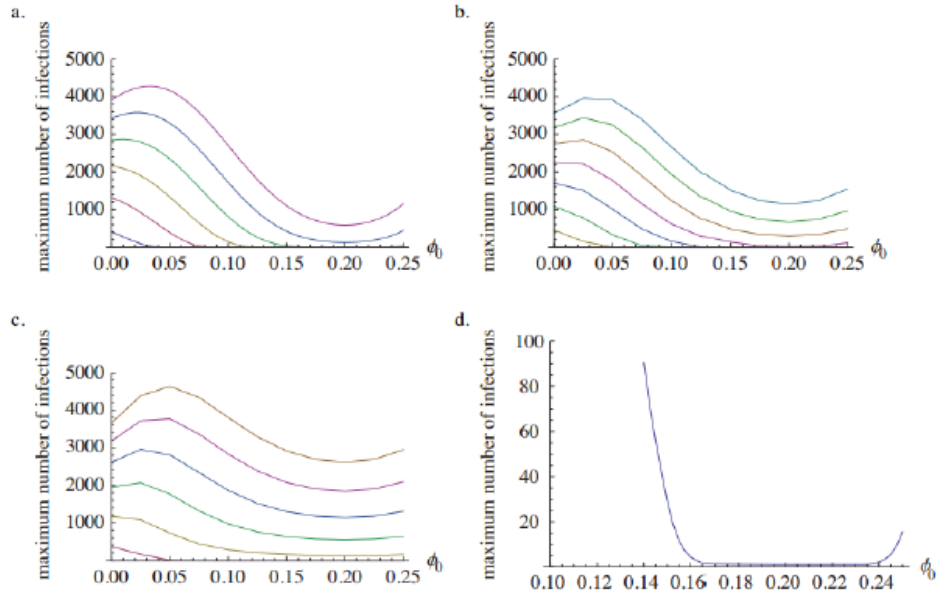

FIG. 4. *In each panel, the peak number of infected individuals is plotted against the fraction ϕ_o, for a range of different values of ζ. Curves are plotted for $\zeta = 2.5 + 0.5n$ for $n = 1, 2, \ldots, 10$.* a. *$\beta_o = 0.5$; curves are plotted for $\zeta = 2.75, 3.75, 4.75, 5.75, 6.75, 7.75$.* b. *$\beta_o = 0.7$; curves are plotted for $\zeta = 2.0, 2.5, 3.0, 3.5, 4.0, 4.5, 5.0$.* c. *$\beta_o = 0.9$; curves are plotted for $\zeta = 2.0, 2.5, 3.0, 3.5, 4.0$.* d. *Zoom-in of panel* a. *for $\zeta = 5.75$ only.*

5.2. The lack of robustness of the homogeneous networks: Case $M = 2$. The simulations we show here are in agreement with the results of Theorem 2. More explicitly, for a fixed γ, we have shown in Theorem 1 that for a homogeneous network (i.e., $\beta_j = \beta_o$ for $j = 1, \ldots, M$) the occurrence of an epidemic depends only on the infection parameter β_o, regardless of the geometry of the network and of the movement of people in the network (i.e., the flux matrix (2.1)). If now we introduce a different infection rate into one of the vertices, the scenario changes completely. In fact, even in the case of a fully connected network with just two nodes, $M = 2$, we observe that the fraction of people between nodes, ϕ_o, could play a crucial role in avoiding an epidemic outbreak.

In the simulations of Figure 5 we set

$$\beta_2 = \beta_o \zeta,$$

where $\zeta > 1$ and the total populations $N_1 = N_2$ are held fixed. The period of integration is 300 weeks. We run several simulations, each for different values of the parameters ϕ_o and β_o. We use the total number of infected individuals, $I_{tot} = I_1 + I_2$, to establish if an epidemic did not occur. In particular, we use the numerical criterion that an epidemic outbreak does not occur if the total number of individuals is less than two.

More explicitly, we can fix ζ and γ and let β_1 vary in a certain interesting domain. This leads us to observe the existence of a critical value $\beta_c = \beta_1^*(\zeta_b)$, such that an epidemic outbreak is expected for all $\phi_o \in [0, 1]$ such that there is no outbreak.

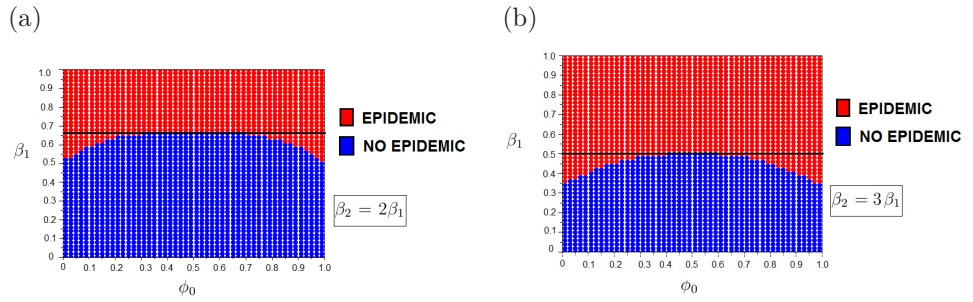

FIG. 5. *The region below the line indicates where no epidemic outbreak is expected. For the criteria of epidemic we use* $\max_{t\in\mathcal{T}}(I_{tot}(t)) \geq 2$, *where* $I_{tot}(t) = I_1(t) + I_2(t)$ *and* $\mathcal{T} = [0, 300]$ *is the simulation interval. We assume* $\gamma = 1$, $\phi_o = [0.01, 1]$, *and initial conditions* $I_1(0) = 1$, $I_2(0) = 0$, $S_1(0) = 9999$, *and* $S_2(0) = 10000$. *We consider the cases* (a) $\beta_2 = 2\beta_1$ *and* (b) $\beta_2 = 3\beta_1$.

6. Data fitting of a dengue fever epidemic outbreak in Rio de Janeiro.

6.1. Introduction. In this section we present a simple application and fitting of the SIR-network model to epidemiological data for the number of dengue fever infections reported in the city of Rio de Janeiro (subsection 6.2) [30]. In particular, we have chosen to examine a period that includes the biggest dengue fever outbreak in the history of the city. In total there were 259392 registered cases and 252 deaths in the whole state of Rio (for further information we recommend [34, 33, 32]).

Rather than considering the whole city of Rio de Janeiro in the simulations, we will consider a small but interesting portion of the whole network consisting of four developed neighborhoods, the center of the city, and a favela. The idea is to partially include the different social patterns of the city. This is done in subsection 6.3. Once the special region is chosen, we need to construct the abstract network. We build up a particular flux matrix (see (2.1) for a definition) inspired by those features that we want to see in the network. This is done in subsection 6.4. After that, in subsection 6.5 we set up some hypotheses on the epidemiological parameters so we can simplify our analysis. In subsection 6.6 we will describe our hypotheses regarding the data and the time period for which the fits will run.

We deduce some values for the epidemiological parameters (both infection and removal rates) by using data fitting through the nonlinear least squares method and using the Scilab function *leastsq*. Briefly, this method tries to find a global minimum point for the *sum of the square residuals (SSR)* with respect to the set of parameters to be fitted $\mathcal{P}$ (i.e., we define a function $SSR = SSR(\mathcal{P})$). For the construction of the SSR function, our methodology was the following: The data of the number of infected individuals of the chosen neighborhoods were placed *side by side* in a single data vector $\boldsymbol{D} := (d_1, d_2, \ldots, d_N)$.[3] The same was done for the numerical solution of the SIR-network model, where a single vector $\bar{\mathbf{I}}(\mathcal{P}) = ((\mathbf{I}(\mathcal{P}))_1, \ldots, (\mathbf{I}(\mathcal{P}))_N)$ was built with the number of infected individuals. Then finally we set

$$SSR(\mathcal{P}) = \sum_{i=1}^{N} \left[\bar{\mathbf{I}}(\mathcal{P})_i - d_i\right]^2.$$

This function SSR indicates how far the numerical solution is from the data points d_i. The function *leastsq* takes an initial value $\mathcal{P}_0$ and finds a minimum point $\mathcal{P}_0^*$ for

[3]Therefore, N = total of time points in the chosen period $\times$ the number of chosen neighborhoods.

SSR. In order to avoid local minimum points, we usually define a grid of different initial values for $\mathcal{P}_0$, and then, among the possibly different values of $\mathcal{P}_0^*$, we choose the one for which we have the smallest SSR.

6.2. Sources of data. The city of Rio de Janeiro is divided by the local government into 159 neighborhoods, which are collected in bigger *administrative regions* (see Figure 6). This classification will be important for the next section. We used data from the city's government that includes the number of newly diagnosed individuals in all neighborhoods. These data have been collected every week since 2006. Figure 7 shows part of one of the tables available from the government website[4] [30].

There is a practical difficulty in addressing the real number of infections, since most of the cases of dengue fever are asymptomatic or the symptoms are similar to those of influenza, for example. In fact, the available data measure only those people who have gone to a hospital to seek medical treatment. Therefore, we can say with certainty that the measurements significantly underestimate the total infected population.

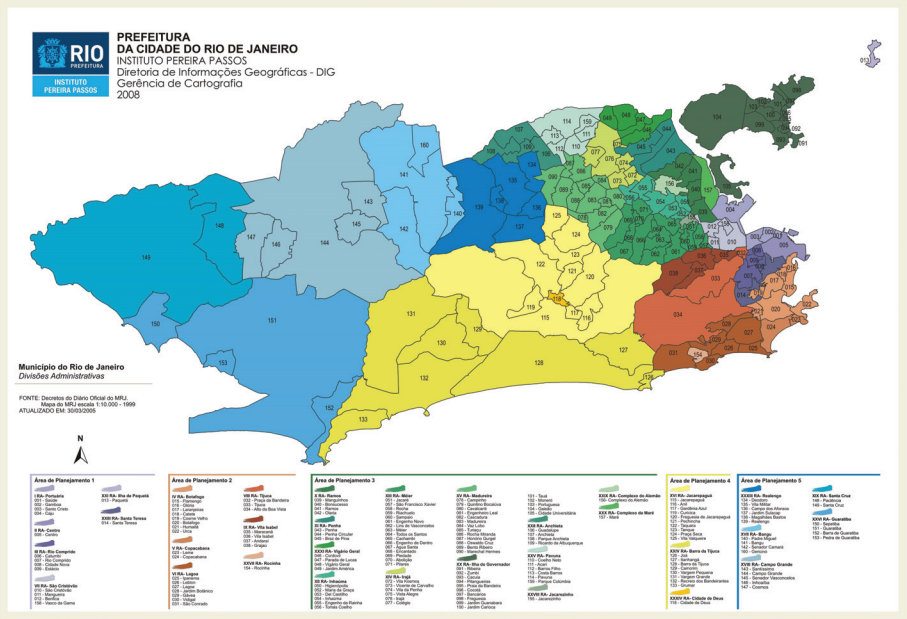

FIG. 6. *Rio de Janeiro divided into neighborhoods (numbered) and administrative regions (colored).*

6.3. The choice of a special region. As is well known, Rio de Janeiro is a huge and complex city: about six and a half million people live in very different conditions (from wealthy neighborhoods to very extensive slums or *favelas*) distributed over a vast area, which includes a variety of hills, forested and planar regions, of about 1260km^2. Our first task is therefore to choose a representative part of the city in order to simplify our analysis. The set of regions we have chosen includes the following:

- A set of 3 administrative regions and 1 neighborhood (called n_1, n_2, n_3, and n_4) which cover the wealthiest parts of the city.

[4] www.rio.rj.gov.br/web/sms.

		Janeiro					Fevereiro				Março			
		01/01/2012 07/01/2012	08/01/2012 14/01/2012	15/01/2012 21/01/2012	22/01/2012 28/01/2012	29/01/2012 04/02/2012	05/02/2012 11/02/2012	12/02/2012 18/02/2012	19/02/2012 25/02/2012	26/02/2012 03/03/2012	04/03/2012 10/03/2012	11/03/2012 17/03/2012	18/03/2012 24/03/2011	25/03/2012 31/03/2012
Áreas de Planejamento, Regiões Administrativas e Bairros	População Censo 2010	Semana 01	Semana 02	Semana 03	Semana 04	Semana 05	Semana 06	Semana 07	Semana 08	Semana 09	Semana 10	Semana 11	Semana 12	Semana 13
TOTAL	6 320 446	953	1 095	1 478	1 652	1 889	2 272	2 758	3 260	4 758	5 767	5 601	6 881	7 262
AREA DE PLANEJAMENTO 1	*297 976*	*38*	*43*	*57*	*62*	*76*	*90*	*72*	*116*	*162*	*165*	*163*	*192*	*202*
I PORTUARIA	48 664	1	2	5	7	11	8	8	16	25	39	29	36	37
SAUDE	2 749	0	0	0	0	2	0	0	2	3	4	2	1	0
GAMBOA	13 108	1	0	2	0	0	3	3	5	7	6	5	6	6
SANTO CRISTO	12 330	0	2	3	3	8	3	3	4	8	11	12	15	15
CAJU	20 477	0	0	0	4	1	2	2	5	7	18	10	14	16
II CENTRO	41 142	6	7	13	10	14	15	14	24	30	33	23	29	37
CENTRO	41 142	6	7	13	10	14	15	14	24	30	33	23	29	37
III RIO COMPRIDO	78 975	9	10	18	14	15	20	24	20	40	31	32	50	47
CATUMBI	12 556	0	0	4	1	2	2	6	3	9	3	6	6	6
RIO COMPRIDO	43 764	6	8	9	10	8	13	11	11	18	23	17	31	28
CIDADE NOVA	5 466	0	0	0	2	0	0	2	3	2	1	2	2	7
ESTÁCIO	17 189	3	2	5	1	5	5	5	3	11	4	7	11	6
VII SÃO CRISTOVÃO	84 908	14	12	14	16	24	36	17	40	51	42	52	63	66
SÃO CRISTOVÃO	26 510	10	8	9	12	15	14	9	26	27	26	21	31	39
MANGUEIRA	17 835	2	1	2	2	5	4	2	5	8	6	17	9	9
BENFICA	25 081	2	3	3	2	4	18	6	9	16	10	14	23	18
VASCO DA GAMA[1]	15 482	0	0	0	0	0	0	0	0	0	0	0	0	0
XXI PAQUETÁ	3 361	1	3	3	1	0	0	1	1	0	1	3	0	1
PAQUETÁ	3 361	1	3	3	1	0	0	1	1	0	1	3	0	1

FIG. 7. *Number of dengue fever cases in Rio de Janeiro for the year* 2012. *Unfortunately, these numbers might represent only a small fraction of the total number of cases. Also shown is the total population for each neighborhood.*

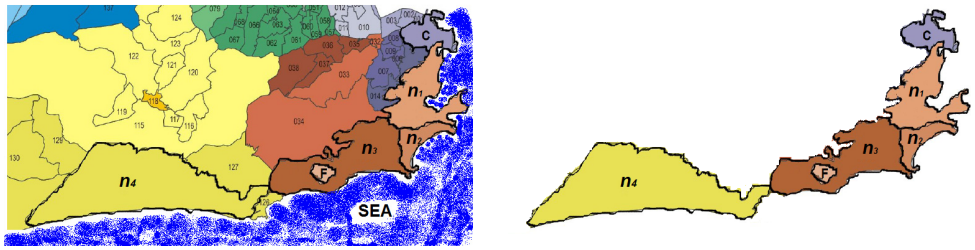

FIG. 8. *Chosen regions that will be the vertices of the network: Administrative region of Botafogo* (n_1)*, administrative region of Copacabana* (n_2)*, administrative region of Lagoa* (n_3)*, neighborhood of Barra da Tijuca* (n_4)*, center neighborhood* (C)*, and favela Rocinha* (F)*. We isolate these regions from the rest of the city.*

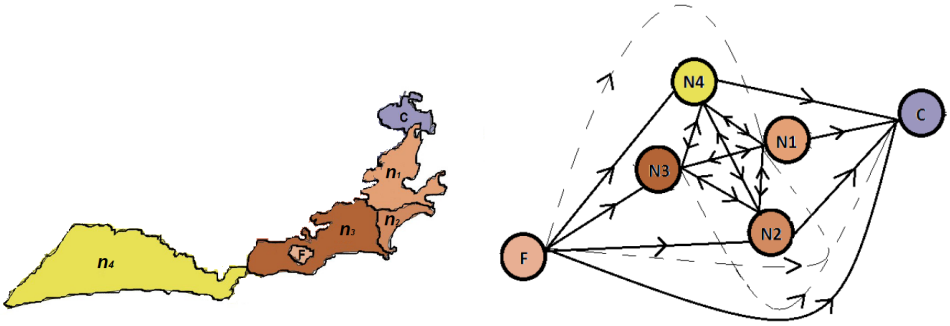

FIG. 9. *A conceptual network is created from the real one.*

- The central part (C) of Rio, where many people go to work every day.
- A huge favela (slum) (F) called Rocinha, situated next to n_1, n_2, n_3, and n_4.

Figures 8 and 9 show the geographical locations and abstract network structure, respectively.

6.4. Building the flux matrix. We must now build a flux matrix $\phi_{6\times 6}$ for the selected regions, so the network will be defined. Such a matrix will take into account

the social structure of regions C, n_1, n_2, n_3, n_4, and F. Therefore, our network must take into account the following:

- People who live in n_1, n_2, n_3, and n_4 usually work either in these regions or in the center (C).
- People who live in the slum (F) may work in the center (C) or in n_1, n_2, n_3, and n_4. On the other hand, extremely few people come from any other neighborhood to work in F, so we set that element of $\phi_{6\times 6}$ to zero.
- People that live in the center of the city (C), on average, rarely leave it to work in other neighborhoods.
- For simplicity, we shall assume that the *residential* neighborhoods n_1, n_2, n_3, and n_4 are equally connected.

We use only two parameters ϕ_o and ϕ_1 to describe the flux matrix. The first represents the fractions of movement between neighborhoods n_1, n_2, n_3, and n_4. The second represents the fraction of movement between any vertex and C. Hence, the flux matrix can be written as

$$\mathbf{\Phi}_{6\times 6} = \begin{array}{c} \\ C \\ n_1 \\ n_2 \\ n_3 \\ n_4 \\ F \end{array} \begin{array}{c} \begin{array}{cccccc} C & n_1 & n_2 & n_3 & n_4 & F \end{array} \\ \begin{pmatrix} 1 & 0 & 0 & 0 & 0 & 0 \\ \phi_1 & \phi_2 & \phi_o & \phi_o & \phi_o & 0 \\ \phi_1 & \phi_o & \phi_2 & \phi_0 & \phi_0 & 0 \\ \phi_1 & \phi_o & \phi_o & \phi_2 & \phi_o & 0 \\ \phi_1 & \phi_o & \phi_o & \phi_o & \phi_2 & 0 \\ \phi_1 & \phi_o & \phi_o & \phi_o & \phi_o & \phi_3 \end{pmatrix} \end{array}. \tag{6.1}$$

By conservation of the fraction of movement (2.2) we must have

$$\phi_2 = 1 - \phi_1 - 3\phi_o \quad \text{and} \quad \phi_3 = 1 - \phi_1 - 4\phi_o.$$

6.5. Epidemiological parameters. We now focus on the epidemiological parameters.

1. We assume that

$$\beta_{n_i} = \beta_0 \quad \forall i \in \{1, 2, 3, 4\}.$$

   This means that all *residential* neighborhoods have the same infection rate. This hypothesis is based on the fact that both local population and government are equally concerned about avoiding stagnant water in private and public places. In fact, control of the proliferation of the *Aedes aegypti* mosquito is influenced by how the local population stores its water and by local health policies. So it is assumed, for example, that people (residents and government) at n_1, n_2, n_3, and n_4 are equally concerned about it.
   We also define the dimensionless factors ζ_1 and ζ_2 such that

$$\beta_C = \zeta_1\beta_0 \quad \text{and} \quad \beta_F = \zeta_2\beta_0.$$

2. We will fit the spatially uniform removal/recovery rate γ. $\frac{1}{\gamma}$ is the viremic period during which an infected individual can transmit the disease to a healthy mosquito.
3. We don't know the values of the fraction parameters ϕ_o and ϕ_1. Thus, our guess is that the percentage of each vertex that leaves home to work in other places is between 20 and 30 percent. Therefore, we will fix these parameters in the set $\{0.05, 0.07\}$.

	C	n_1	n_2	n_3	n_4	F
Total Population (approximately)	30.000	230.000	160.000	180.000	120.000	70.000
Initially infected Population (x 10)	0	20	30	40	0	10

FIG. 10. *Total population (N_i) of each neighborhood considered in our simulations. Also listed is the initially infected population ($I_i(0)$), which we multiply by* 10. *Here $i \in \{C, n_1, n_2, n_3, n_4, F\}$. This constant factor is due to the problem of obtaining the real number of dengue cases.*

These considerations have led us to the following.

DEFINITION. *The element $\mathcal{P} := (\beta_0, \zeta_1, \zeta_2, \gamma)$ is the vector of parameters to be fitted.*

6.6. Hypotheses on the data.

1. The number of infected humans given by the government is here multiplied by 10, including the initial number of cases at the start of the considered time period (see Figure 10). An explanation for this factor of 10 is the following: We estimate that 90% of the cases are asymptomatic or sufficiently mild that medical attention is not sought. This hypothetical percentage is reasonable for our proposes. However, it is not clear how to determine the precise proportion of asymptomatic cases. See [10] for references. For people with classic symptoms of dengue fever (mild fever, headache, muscle pains) there are no recommendations other than rest and hydration (see [37]).
2. The data of the 6 vertices are arranged in a single array. The time period here is 60 weeks and runs from October, 2007 to December, 2008.[5] Hence, it covers the whole period of the biggest epidemic outbreak within the past 20 years in the city of Rio de Janeiro. Figure 11 shows how data are arranged for the fitting process. The numbers of infected individuals from each of the 6 neighborhoods (multiplied by the factor 10) are placed side by side in a single vector $\boldsymbol{D} := (d_1, d_2, \ldots, d_{366})$.

6.7. Results. As we stated earlier, the goal of this section is to deduce the infection parameters and to draw some conclusions about the reliability of the SIR-network model for the regions considered. In addition, we would like to check whether such a simplified model can provide useful insight into the conditions for an epidemic outbreak to and how to avoid it or control it. The results are shown in Figure 12 and summarized as follows:

1. **The center (C) and the favela (F) exhibit higher infection rates**. We observed that $\zeta_1 > 1$ and $\zeta_2 > 1$. This means that $\beta_C > \beta_0$ and $\beta_F > \beta_0$.

[5]Specifically, from October 10, 2007 to December 3, 2008.

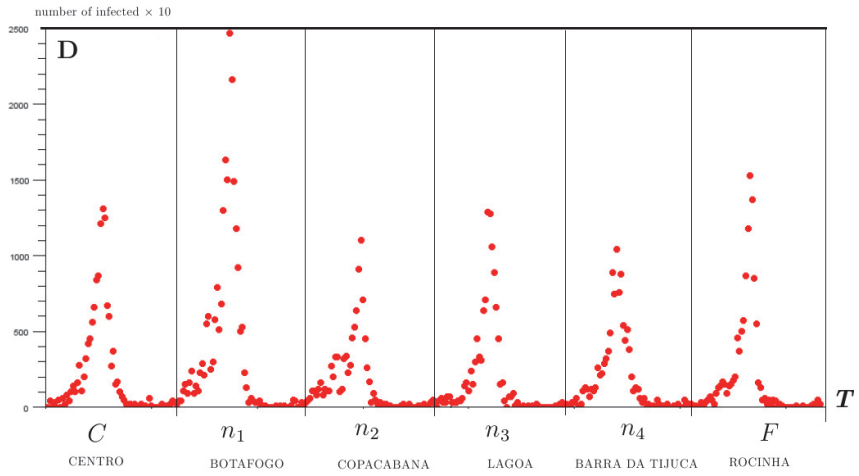

FIG. 11. *We set the data for the period from October,* 2007 *to December,* 2008 *in the form* $\boldsymbol{T} \times \mathbf{D}$*, where* $\boldsymbol{T} = (1, 2, \ldots, 366)$*. We multiply all numbers of incident cases by* 10 *and create the respective data vector* $\mathbf{D} = (d_1, d_2, \ldots, d_{366})$*.*

In particular, we see that $\beta_{n_i} = \beta_0 < \gamma$ in all three simulations, which shows that these vertices would independently avoid an epidemic if they were not linked to the center and the slum.

2. **The center is more "infectious" than the favela**. We also notice that $\zeta_1 > \zeta_2$, which means that $\beta_C > \beta_F$ in all simulations. Thus, we conclude that the special position of C, together with a high infection rate, contributes to the epidemic outbreak in the whole network. This reinforces the importance of good mosquito suppression in this core neighborhood.
3. **Good accuracy in estimating the removal rate γ**. It is known that the average infectious period for dengue is about 4 or 5 days [37]. We know that for the SIR-network, this quantity is given by $\tau = \frac{1}{\gamma}$ [32]. This information should give us $\gamma \in [1.4, 1.75]$. Our fitting gives us an estimate for γ that is close to this interval. In fact, the best fit (lowest *SSR*) gives us $\gamma = 1.55$. This shows that this implementation of the SIR-network model gives a result that is consistent with previous studies.

7. Data fitting for Gaussian time-dependent infection rates. We observe that the fits achieved in the previous section underestimate the peak incidence. Since the transmission parameters implicitly include the density of mosquitoes in each neighborhood, it is natural to consider a time-varying transmission coefficient that can roughly model the effects of the climate. The summer period is known to be the peak period for mosquitoes, and this is likely due to high rainfall which creates many breeding sites in stagnant water. We will therefore model the infection parameters β_i as a set of floor Gaussian functions,

$$\beta_i(t) = \frac{\eta_i}{\sigma_i\sqrt{2\pi}} \exp\left(-\frac{(t-\mu_i)^2}{2\sigma_i^2}\right) + f_i, \tag{7.1}$$

where $\eta_i \geq 0$, $\sigma_i > 0$, $\mu_i \geq 0$, and $f_i \geq 0$ are constant terms representing the peak transmissibility, mean and variance around the peak time, and the floor infection rate

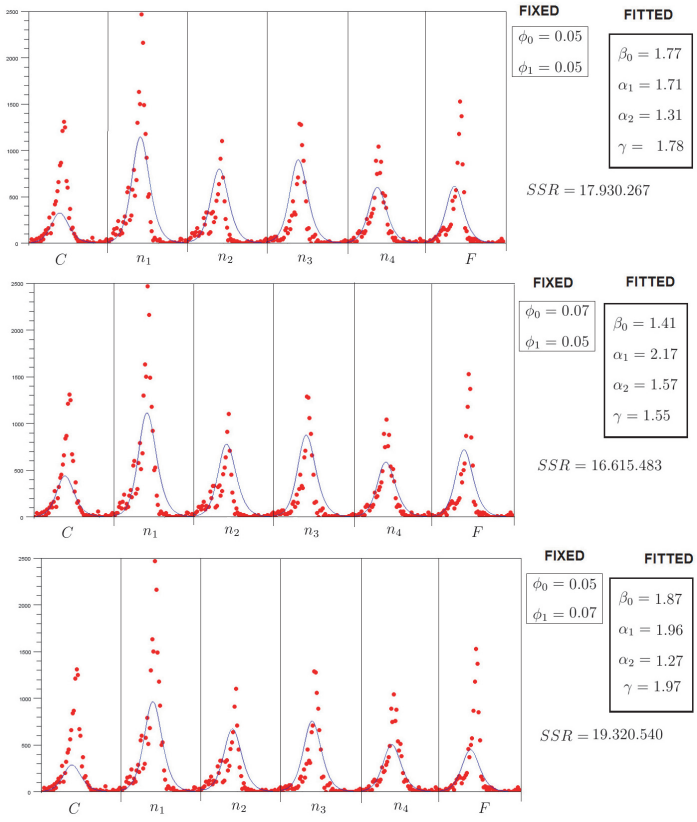

FIG. 12. *Dots represent the data (×10) given by the government of Rio de Janeiro. Lines indicate the numerical solution for the modified SIR-network such that the SSR function for a nonlinear least squares method is minimized. Here we consider three cases for the fraction parameters:* $\phi_o = 0.05$ *and* $\phi_1 = 0.05$, $\phi_o = 0.07$ *and* $\phi_1 = 0.05$, $\phi_o = 0.05$ *and* $\phi_1 = 0.07$.

(see Figure 13). The equations of the SIR-network model are now written as

$$\dot{S}_i(t) = -\sum_{j=1}^{M}\sum_{k=1}^{M} \beta_j(t)\phi_{ij} S_i \frac{\phi_{kj} I_k}{N_j^p}, \tag{7.2}$$

$$\dot{I}_i(t) = \sum_{j=1}^{M}\sum_{k=1}^{M} \beta_j(t)\phi_{ij} S_i \frac{\phi_{kj} I_k}{N_j^p} - \gamma I_i, \tag{7.3}$$

$$\dot{R}_i(t) = \gamma I_i. \tag{7.4}$$

7.1. Analysis of the data fitting. Here we will adopt the same data fitting approach as in the previous section and use the same simplified network of neighborhoods described above. To simplify our analysis, we choose positive constants η, σ, μ, f, ζ_1, ζ_2, γ such that

$$\beta_{ni}(t) = \frac{\eta}{\sigma\sqrt{2\pi}} \exp\left(-\frac{(t-\mu)^2}{2\sigma^2}\right) + f \quad \forall i \in \{1,2,3,4\}$$

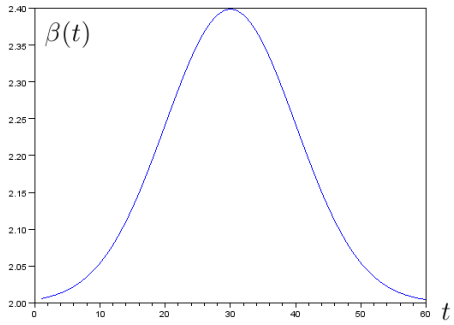

FIG. 13. *Gaussian $\beta(t)$ for $\eta = 10$, $\mu = 30$, $\sigma = 10$, and $f = 2$.*

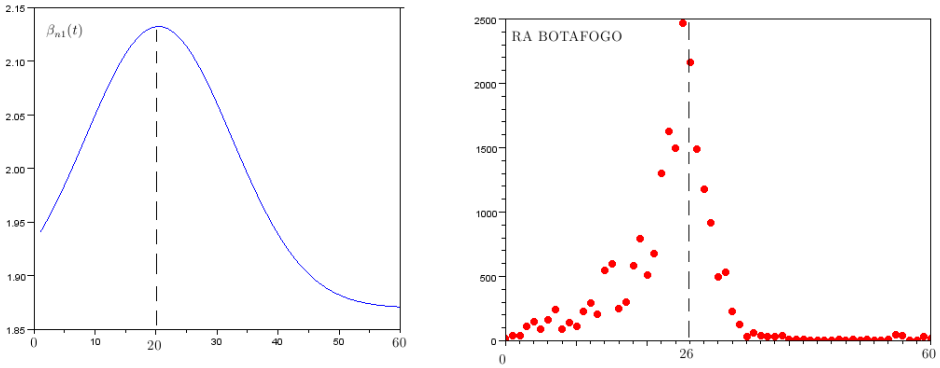

FIG. 14. *The time gap between predicted (fit) peaks of infection rates and reported infections for the administrative region of Botafogo. The first occurs during week* 20 *and the second occurs* 6 *weeks later. This illustrates the first insight into the Gaussian infection rate model.*

is the infection rate of the neighborhood n_i at time t. For the center vertex C and slum F we set

$$\beta_C(t) = \frac{\zeta_1 \eta}{\sigma\sqrt{2\pi}} \exp\left(-\frac{(t-\mu)^2}{2\sigma^2}\right) + f \quad \text{and} \quad \beta_F(t) = \frac{\zeta_2 \eta}{\sigma\sqrt{2\pi}} \exp\left(-\frac{(t-\mu)^2}{2\sigma^2}\right) + f.$$

These assumptions lead us to the following.

DEFINITION. *The set $\mathcal{P} := \{\eta, \sigma, \mu, f, \zeta_1, \zeta_2, \gamma\}$ is the set of parameters to be fitted.*

We then proceed as we did for the constant β case. The results are shown in Figures 14, 15, and 16, and we draw the following conclusions.

1. **Time-varying transmissibility leads to improved fits of the incidence.** It can be immediately seen that the Gaussian time dependency for the β_i's produces better fits, especially in terms of capturing the peak incidence and the late-stage decline of the epidemic. This confirms that it is reasonable to assume that there was a period of higher infectiousness. For dengue fever we can perhaps understand it as a period with higher numbers of the *Aedes aegypti* mosquito.
2. **The predicted highest value for the infection rate occurs during the summer and precedes the peak incidence.** We remind the reader that

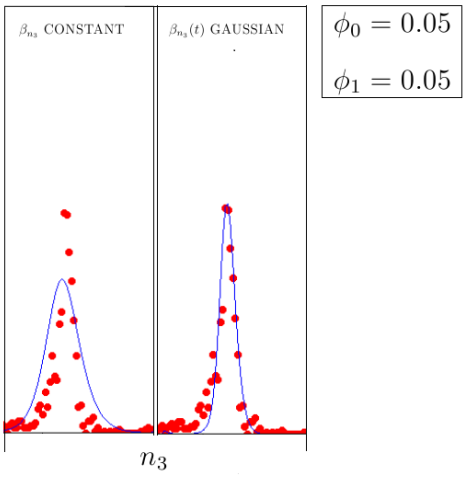

FIG. 15. *Difference between fits for the constant and Gaussian β_i for vertex n_3 (administrative region of Lagoa). For the Gaussian case, both the peak and the final stages of the outbreak are well fitted.*

the set of data covers the period from October, 2007 to December, 2008. We observe a difference of 6–8 weeks between the peak in the number of infected individuals and the peak of the transmissibility parameters $\beta_j(t)$. Figure 14 shows this difference for a residential neighborhood (n_1) in one of the simulations. In all simulations, the maximum transmissibility is achieved at about 19–20 weeks (from January to February), while the peak in the number of infected individuals is found to occur after that, during weeks 26–28 (from March to April).

How can we understand such a delay? Due to the complexity of dengue transmission and modeling limitations, a precise explanation of all phenomena is not possible at present. However, there are several factors which we believe could play a major role in causing the sudden peaks in the transmission rates. From the perspective of an enhanced population of mosquitoes, January and February are high-temperature months. The relationship between temperature and mosquito density has been studied, and it is known that there is an increased production of eggs associated with higher temperatures [23]. Another point is the abundance of rainfall in the period from December, 2006 to April, 2007 in Rio de Janeiro. In December there occurred sporadic heavy rains, while from March to April there was the usual rainy season (with higher humidity, also recorded during these two months). This would have facilitated the accumulation of water in containers, contributing to the proliferation of the main vector of dengue, the *Aedes aegypti* mosquito.

Finally, from the perspective of human population dynamics, we believe that the huge incoming flux of tourists in the summer—in particular during the carnival period in February—could temporarily impact the dynamics of dengue, as those tourists effectively increase the city's healthy population, and thus may contribute to accelerate the spread of dengue. In fact, during the carnival period the local population of the city increases by a factor of 16–20% (about one million tourists in a population of about six million). For

$$\beta_{ni}(t) = \frac{\eta}{\sigma\sqrt{2\pi}} \exp\left(-\frac{(t-\mu)^2}{2\sigma^2}\right) + f \qquad \beta_C(t) = \frac{\zeta_1\eta}{\sigma\sqrt{2\pi}} \exp\left(-\frac{(t-\mu)^2}{2\sigma^2}\right) + f$$

$$\forall i \in \{1,2,3,4\} \qquad \beta_F(t) = \frac{\zeta_2\eta}{\sigma\sqrt{2\pi}} \exp\left(-\frac{(t-\mu)^2}{2\sigma^2}\right) + f.$$

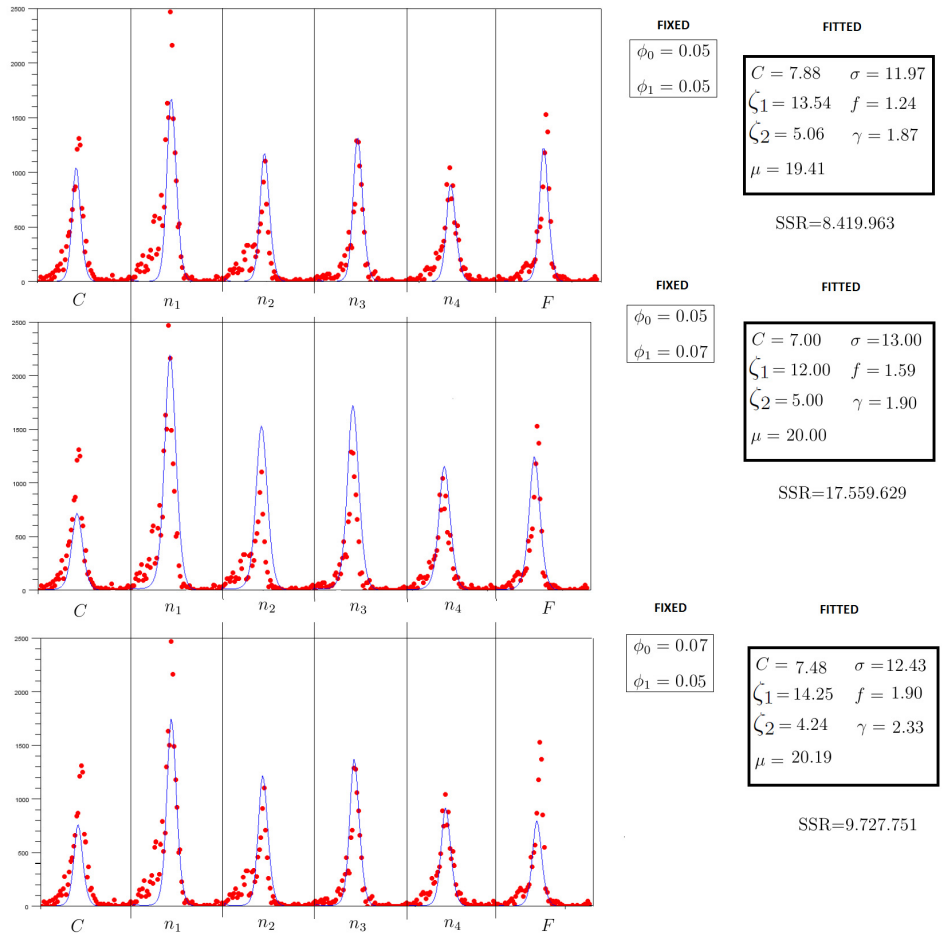

FIG. 16. *Results for the Gaussian infection rate case. Dots represent the data (×10) given by the government of Rio de Janeiro. The lines indicate the numerical solution for the modified SIR-network such that the SSR function for a nonlinear least squares method is minimized. Here we consider three cases for the fraction parameters:* $\phi_o = 0.05$ *and* $\phi_1 = 0.05$, $\phi_o = 0.07$ *and* $\phi_1 = 0.05$, $\phi_o = 0.05$ *and* $\phi_1 = 0.07$.

the city of Recife (in the state of Pernambuco), a study done by Fundação Oswaldo Cruz (Fiocruz) [6] reported that about 90% of the local population had already contracted dengue. If the same were true for Rio de Janeiro's population, the sudden arrival of a mass of healthy tourists would have an important impact on the epidemic dynamics.

3. **The center is more "infectious" than the favela again.** Again, our model fitting shows that the nodes C and F have the highest infection rates: ζ_1,$\zeta_2 > 1$. Moreover, $\zeta_1 > \zeta_2$ in all simulations. As in the constant β_i case, we retain the conclusion that the center is the most important node in terms of the epidemic outbreak.

8. Conclusions. In this paper we have presented analytical results for a simplified epidemiological model suitable for a vector-borne disease such as dengue fever. Specifically, we established epidemic thresholds for homogeneous and mildly heterogeneous networks in terms of the transmissibility and infectious period of the disease at each node in the network. The main observation, from the theoretical point of view, is that a homogeneous network is not robust in the sense that an inhomogeneity in one node can drastically change the system behavior. We saw in Lemma 1 of section 4.1 that for homogeneous networks, the geometry of the network and the fractions of movement played no role in determining R_o and that, in this respect, a homogeneous network is equivalent to a single node system. Once we examined a single inhomogeneity in one single node, we found conditions on the inhomogeneity and the fractions of movement that control the stability of the system and the possibility of an epidemic. An important fact is that even when there is the potential for an epidemic based on transmission in a single node, the epidemic-prone state can be avoided by controlling the movement of people among nodes. This can be understood by viewing the movement of people as a dilution of the infected population in a given (troublesome) node.

From a practical point of view, the SIR-network model performs well in fitting the data of dengue fever in Rio de Janeiro. Centered nodes with higher infection rates are found to be the most important drivers of the epidemic outbreaks. When a time-dependent infection rate is introduced, we see how its peak precedes the peak of detected infections. Moreover, the time gap between these two peaks highlights the importance of the summer period in Rio in influencing infection rates. We believe that this is mostly due to temperature variations and to the abundance of rainfall, with the consequent development of pools of stagnant water. Both factors help in the proliferation of the *Aedes aegypti* mosquito. The carnival period, with its huge increase in the local population, could also play an important role, and our model could be extended to better take this into account.

In the SIR-network model, we do not explicitly take into consideration the dynamics of the vector population and of the disease-host interaction, as done in other models. These dynamics are effectively hidden within the infection parameter β. This hypothesis facilitates the theoretical analysis, allowing us to focus on finding interesting insights about the influence of the movement of people on the epidemic dynamics. However, the time scales of vector turnover and of dengue-vector interaction are not sufficiently rapid compared to the duration of the epidemic, so we would not expect them to be completely negligible (mosquitoes become infectious only after an incubation period, typically on the order of weeks, and can then remain infectious for life; infected humans are also not immediately infectious to mosquitoes [9]). It would be interesting to include vector dynamics in the model, and hence investigate in which dynamical regimes we would find qualitatively similar results.

Appendix. Proof of Theorem 2. The goal is to find conditions on parameters such that all the eigenvalues of the next generation matrix $\mathcal{C}$ are within the unit circle, so that $R_o < 1$. At the start of the epidemic, the basic SIR-network system reduces to

$$\mathcal{K}_{ij} = \frac{1}{\gamma} \sum_{j=1}^{M} \beta_j \phi_{ij} \phi_{kj}$$

since the number of infected people at a node is extremely small, and so the number of susceptible individuals is equal to the total population. Applying the definition of the fractions of movement for a fully connected network, we obtain

$$\begin{aligned}
\mathcal{K} &= \frac{\beta_o}{\gamma} \begin{pmatrix} p+c_1 & q & q & \dots & \dots & q \\ q & p+c_o & p & \dots & \dots & p \\ q & p & p+c_o & \dots & \dots & p \\ \vdots & \vdots & \vdots & \vdots & \vdots & \vdots \\ \vdots & \vdots & \vdots & \vdots & p+c_o & p \\ q & p & p & \dots & p & p+c_o \end{pmatrix} \\
&= \frac{\beta_o}{\gamma} \begin{pmatrix} p & q & q & \dots & \dots & q \\ q & p & p & \dots & \dots & p \\ q & p & p & \dots & \dots & p \\ \vdots & \vdots & \vdots & \vdots & \vdots & \vdots \\ \vdots & \vdots & \vdots & \vdots & p & p \\ q & p & p & \dots & p & p \end{pmatrix} + \frac{\beta_o}{\gamma} \begin{pmatrix} c_1 \\ c_o \\ c_o \\ \vdots \\ \vdots \\ c_o \\ c_o \end{pmatrix} I \\
&= \frac{\beta_o}{\gamma} \left(\mathcal{P} + \mathcal{D} \right).
\end{aligned}$$

Here we have defined $p = \phi_o(2 + (\zeta - M - 1)\phi_o)$, $q = \phi_o(1 - \phi_o + \zeta(1 - (M-1)\phi_o))$, $c_o = (M\phi_o - 1)^2$, and $c_1 = (M\phi_o - 1)(2\phi_o + \zeta((M-2)\phi_o - 1))$. It is immediately apparent that the matrix $\mathcal{P}$ has rank two, and therefore the matrix $\mathcal{K}$, expressed as the sum of a low-rank matrix and a diagonal matrix, is amenable to the diagonal expansion method (see, e.g., Collings [11]). This expansion allows us to write the characteristic polynomial for the eigenvalues λ of $\mathcal{P} + \mathcal{D}$, i.e.,

$$|\mathcal{P} + \mathcal{D} - \lambda I| = |\mathcal{P} + \mathcal{D}'|,$$

where $\mathcal{D}' = \mathcal{D} - \lambda I$. As described by Collings, the characteristic polynomial can be expanded as a summation over all possible submatrices,

$$|\mathcal{D}' + \mathcal{P}| = \sum_{\theta \subset \mathcal{S}} |D'(\bar{\theta})| \cdot |\mathcal{P}(\theta)|.$$

The notation here is as follows: Define $S = \{1, 2, \dots, M\}$. Then for any subset $\theta \subset S$, define $\bar{\theta} = S \setminus \theta$ as the complement of θ in S. Finally, for an $M \times M$ matrix called A, let $A(\theta)$ be the submatrix where all rows and columns not indexed in θ are deleted.

In our case, $\mathcal{P}$ has rank two, so all submatrices bigger than 2×2 have determinant zero. This greatly simplifies the summation, and we are able to find the characteristic polynomial of $\mathcal{P} + \mathcal{D}$ in the simplified form

$$(c_o - \lambda)^{M-2} \left[\lambda^2 - (c_0 + c_1 + pM)\lambda + (c_1 c_o + p(M-1)c_1 + pc_o + (M-1)(p^2 - q^2)) \right] = 0.$$

Therefore, $\mathcal{K}$ has an eigenvalue $\frac{\beta_o}{\gamma} c_o = R_o^{\text{hom}}(M\phi_o - 1)^2$ of multiplicity $M-2$, while the quadratic term (in square brackets) determines the other two eigenvalues.

The first condition for stability is that

$$R_o^{\text{hom}}(M\phi_o - 1)^2 < 1. \tag{A.1}$$

Since we know that $0 < \phi_o \leq \frac{1}{M-1}$, this condition is automatically satisfied for all M provided $R_o^{\text{hom}} < 1$. We can also observe that it is always possible to satisfy this condition, even if $R_o^{\text{hom}} > 1$, by choosing $M\phi_o$ close enough to 1, while simultaneously obeying the constraint $M\phi_o \leq \frac{M}{M-1}$.

We also require that the other two eigenvalues (roots of the quadratic term) lie within the unit circle. This can be tested by applying the Jury conditions [27] to the quadratic equation. For a quadratic equation $P(\lambda) = \lambda^2 + a_1\lambda + a_o = 0$, these conditions are $P(1) = 1 + a_1 + a_o > 0$, $P(-1) = 1 - a_1 + a_o > 0$, and $P(0) = a_o < 1$. For our system, this reduces to

$$\Big\{R_o^{\text{hom}}\Big[\zeta\Big(R_o^{\text{hom}}(M\phi_o-1)^2 - (M-1)\phi_o(M\phi_o-2) - 1\Big) + \phi_o(2-M\phi_o) - 1\Big] + 1\Big\} > 0, \tag{A.2}$$

$$\Big\{R_o^{\text{hom}}\Big[\zeta\Big(R_o^{\text{hom}}(M\phi_o-1)^2 + (M-1)\phi_o(M\phi_o-2) + 1\Big) - \phi_o(2-M\phi_o) + 1\Big] + 1\Big\} > 0, \tag{A.3}$$

$$(R_o^{\text{hom}})^2\zeta(M\phi_o - 1)^2 < 1. \tag{A.4}$$

Examination of condition (A.3) shows that it is always satisfied, since the first term in square brackets is certainly positive, and $-\phi_o(2-M\phi_o)+1 = 1 - 2\phi_o + M(\phi_o)^2 \geq 1 - \frac{2}{M-1} + M(\phi_o)^2 > 0$ since $0 \leq \phi_o \leq 1/(M-1)$.

The remaining conditions (A.1), (A.2), (A.4) are difficult to understand in full generality. For that reason, we will analyze a number of special cases.

Case 1: $R_o^{hom} = 1$. This case corresponds to there being $M-1$ neighborhoods that are "just stable" from the point of view of epidemic spread. In this case, our stability conditions reduce to the following simple form:

$$\begin{aligned}(M\phi_o - 1)^2 &< 1,\\ (\zeta - 1)\phi_o(M\phi_o - 2) &> 0,\\ \zeta(M\phi_o - 1)^2 &< 1.\end{aligned}$$

(1) If $\zeta < 1$, then the conditions reduce to the following simple condition:

$$|M\phi_o - 1| < 1,$$

which is satisfied since we required that the matrix $\mathcal{C}$ be positive definite. This makes sense; if all the nodes are stable individually, then the network is also stable.

(2) If $\zeta > 1$, then it is impossible to satisfy the conditions (the second condition implies that $M\phi_o > 2$). This indicates that a network of nodes that individually are marginally stable ($R_o^{\text{hom}} = 1$) can be destabilized by a perturbation in a single node.

Case 2: $R_o^{hom} < 1$. Based on the previous case, we should ask how unstable the single perturbed node needs to be to lead to an epidemic.

(1) *Weakly connected network*. Suppose $\phi_o \ll 1$ and expand the conditions in powers of ϕ_o, retaining only the first order terms. Working in this regime, we have

conditions

$$-1 < (R_o^{\text{hom}})^2\zeta(1-2M\phi_o) < 1,$$
$$(1-R_o^{\text{hom}}) - R_o^{\text{hom}}(2\phi_o(\zeta-1)+\zeta(1-R_o^{\text{hom}})(1-2M\phi_o)) > 0.$$

These can be rephrased to highlight the requirements on ζ for stability:

$$\zeta < \frac{1}{(R_o^{\text{hom}})^2 - 2M(R_o^{\text{hom}})^2\phi_o},$$
$$\zeta < \frac{(1-R_o^{\text{hom}})+2\phi_o R_o^{\text{hom}}}{R_o^{\text{hom}}((1-R_o^{\text{hom}})(1-2M\phi_o)+2M\phi_o)}.$$

In the limit $\phi_o \to 0$, these conditions become $\zeta < 1/(R_o^{\text{hom}})^2$ and $\zeta < 1/R_o^{\text{hom}}$, respectively. The latter condition is more restrictive in this case when $R_o^{\text{hom}} < 1$ and is as expected; that is, a stable disconnected network requires that $R_o^{\text{hom}} < 1$ in every node individually.

(2) *Strongly connected network.* The maximum possible value of ϕ_o is $1/(M-1)$. So we can study a network with strong connections by setting $\phi_o = 1/M$. In this scenario, the single stability condition is

$$(1-R_o^{\text{hom}}) + R_o^{\text{hom}}\frac{1-\zeta}{M} > 0$$

which is satisfied whenever

$$\zeta < 1 + \frac{1-R_o^{\text{hom}}}{R_o^{\text{hom}}}M,$$

or perhaps it is clearer to focus on the stability condition for the actual R_o in the perturbed node:

$$R_o^{\text{p}} = \zeta R_o^{\text{hom}} < R_o^{\text{hom}} + (1-R_o^{\text{hom}})M.$$

This formula clearly indicates the contribution to instability arising from the surrounding population of stable nodes.

Case 3: $R_o^{hom} > 1$. In this case, we would examine the conditions on the perturbed node that stabilize an otherwise unstable set of nodes. We omit the description of this case, as it is not what we are interested in.

ϕ_o conditions: Suppose that $R_o^{\text{hom}} < 1$, $\zeta > 1/R_o^{\text{hom}} > 1$, and $M > 2$ are fixed. Can we find bounds on ϕ_o that guarantee the system is stable? We already have that $\phi_o < 1/(M-1)$. By rearranging stability condition (A.2) and focusing on ϕ_o, we can establish the following range that guarantees stability:

$$\phi_o \in \left(\max\left\{0, \frac{1}{M} - \tilde{\phi}\right\}, \min\left\{\frac{1}{M-1}, \frac{1}{M} + \tilde{\phi}\right\}\right),$$

where

$$\tilde{\phi} = \frac{1}{M}\sqrt{\frac{M(1-R_o^{\text{hom}}) - R_o^{\text{hom}}(\zeta-1)}{R_o^{\text{hom}}\left(M\zeta(1-R_o^{\text{hom}}) - (\zeta-1)\right)}}.$$

For this condition to make sense, we require that $\zeta > 1 + M(1-R_o^{\text{hom}})/R_o^{\text{hom}}$, and this condition on ζ defines a general minimum value that allows epidemics to occur irrespective of ϕ_o. ∎

From the theorem, one of the conditions that is necessary (but not sufficient) to prevent the possibility of epidemics is that

$$\zeta < 1 + \frac{(1 - R_o^{\text{hom}})}{R_o^{\text{hom}}} M.$$

We rewrite this formula as $R_o^{\text{avg}} < 1$, where

$$R_o^{\text{avg}} = \frac{1}{M} \frac{\sum_{i=1}^{M} \beta_i}{\gamma} = \frac{(M-1)}{M} R_o^{\text{hom}} + \frac{\zeta \beta_0}{M\gamma} < 1$$

since $\beta_i = \beta_0$ for all $i \in V \backslash \{2\}$. Therefore, we can conclude that whenever the *average* reproductive number, averaged over all nodes, is less than unity, the disease-free equilibrium can be stable or unstable, depending on movement among the nodes. Whether an epidemic can occur can be determined by checking whether the movement parameter ϕ_o is in the interval $\mathcal{I}$ defined in the theorem.

Acknowledgments. We express our thanks to Jorge Pacheco, Francisco Santos, Pedro Younes, and Renata Stella Khouri for very insightful contributions to the initial formulation of the model [5]. We are also grateful to Bernard Cazelles, Nildimar Honorio, and Claudia Codeço for helpful discussions about the epidemiology of dengue fever.

REFERENCES

[1] B. Adams and D.D. Kapan, *Man bites mosquito: Understanding the contribution of human movement to vector-borne disease dynamics*, PLoS ONE, 4 (2009), e6763. doi: 10.1371/journal.pone.0006763.

[2] J. Arino and P. van den Driessche, *A multi-city epidemic model*, Math. Pop. Stud., 10 (2003), pp. 175–193. doi:10.1080/08898480306720.

[3] C. Atkinson and G.E.H. Reuters, *Deterministic epidemic waves*, Math. Proc. Cambridge Philos. Soc., 80 (1976), pp. 315–330. doi:10.1017/S0305004100052944.

[4] S. Bhatt, P.W. Gething, O.J. Brady, J.P. Messina, A.W. Farlow, C.L. Moyes, J.M. Drake, J.S. Brownstein, A.G. Hoen, O. Sankoh, M.F. Myers, D.B. George, T. Jaenisch, G.R.W. Wint, C.P. Simmons, T.W. Scott, J.J. Farrar, and S.I. Hay, *The global distribution and burden of dengue*, Nature, 496 (2013), pp. 504–507. doi:10.1038/nature12060.

[5] S. Boatto, L.M. Stolerman, J. Pacheco, F. Santos, and R.S. Khouri, *SIR-Network Model for Epidemics Dynamics in a City*, in preparation.

[6] C. Braga, C.F. Luna, C.M.T. Martelli, W. Viera de Souza, M.T. Cordeiro, N. Alexander, M.F.P. Militão de Albuquerque, J.C. Silveira Júnior, and E.T. Marques, *Seroprevalence and risk factors for dengue infection in socio-economically distinct areas of Recife, Brazil*, Acta Tropica, 113 (2010), pp. 234–240. doi: 10.1016/j.actatropica.2009.10.021.

[7] Centers for Disease Control and Prevention, *Dengue and the Albopictus Mosquito,* http://www.cdc.gov/dengue/resources/30Jan2012/albopictusfactsheet.pdf.

[8] L. C'esar de Castro Medeiros, C.A. Rodrigues Castilho, C. Braga, W. Viera de Souza, L. Regis, and A.M. Vieira Monteiro, *Modeling the dynamics transmission of dengue fever: Investigating disease persistence*, PLoS Negl. Trop. Dis., 5 (2011), pp. 1–14. doi: 10.1371/journal.pntd.0000942.

[9] M. Chan and M.A. Johansson, *The incubation periods of dengue viruses*, PLoS ONE, 7 (2012), e50972. doi:10.1371/journal.pone.0050972.

[10] C. Chastel, *Eventual role of asymptomatic cases of dengue for the introduction and spread of dengue viruses in non-endemic regions*, Front Physiol., 3 (2012). doi:10.3389/fphys.2012.00070.

[11] B.J. Collings, *Characteristic polynomials by diagonal expansion*, Amer. Statist., 37 (1983), pp. 233–235. doi:10.1080/00031305.1983.10483111.

[12] O. Diekmann and J.A.P. Heesterbeek, *Mathematical Epidemiology of Infectious Diseases: Model Building, Analysis and Interpretation*, John Wiley and Sons, Chichester, UK, 2000.
[13] O. Diekmann, J.A.P. Heesterbeek, and J.A.J. Metz, *On the definition and the computation of the basic reproduction ratio R_o in models for infectious diseases in heterogeneous populations*, J. Math. Biol., 28 (1990) pp. 365–382. doi:10.1007/BF00178324.
[14] P. van den Driessche and J. Watmough, *Reproduction numbers and sub-threshold endemic equilibria for compartmental models of disease transmission*, Math. Biosci., 180 (2002), pp. 29–48. doi:10.1016/S0025-5564(02)00108-6.
[15] F. Dubault, *Dengue à Nîmes: 4 nouveaux cas suspects sous surveillance*, FranceTV 3, 2015. http://france3-regions.francetvinfo.fr/languedoc-roussillon/gard/nimes/dengue-nimes-4-nouveaux-cas-suspects-sous-surveillance-791049.html.
[16] G.R. Fulford, M.G. Roberts, and J.A.P. Heesterbeek, *The metapopulation dynamics of an infectious disease: Tuberculosis in possums*, Theor. Popul. Biol., 61 (2002), pp. 15–29.
[17] L.C. Harrington, T.W. Scott, K. Lerdthusnee, R.C. Coleman, A. Costero, G.G. Clark, J.J. Jones, S. Kitthawee, P. Kittayapong, R. Sithiprasasna, and J.D. Edman, *Dispersal of the dengue vector Aedes aegypti within and between rural communities,* Am. J. Trop. Med. Hyg., 72 (2005), pp. 209–220.
[18] J.A.P. Heesterbeek, *R_o*, Ph.D. Thesis, University of Leiden, Leiden, The Netherlands, 1992.
[19] R. A. Horn and C.R. Johnson, *Matrix Analysis*, Cambridge University Press, Cambridge, UK, 1987.
[20] Y. Li, F. Kamara, G. Zhou, S. Puthiyakunnon, C. Li, Y. Liu, Y. Zhou, L. Yao, G. Yan, and X.-G. Chen, *Urbanization increases Aedes albopictus larval habitats and accelerates mosquito development and survivorship*, PLoS Negl. Trop. Dis., 8 (2014), e3301. doi:10.1371/journal.pntd.0003301.
[21] M.J. Keeling, L. Danon, M.C. Vernon, and T.A. House, *Individual identity and movement networks for disease metapopulations*, Proc. Natl. Acad. Sci. USA, 107 (2010), pp. 8866–8870. doi:10.1073/pnas.1000416107.
[22] W.O. Kermack and A.G. McKendric, *A contribution to the mathematical theory of epidemics*. 1, Proc. Roy. Soc. Ser. A, 115 (1927), pp. 700–721. doi:10.1098/rspa.1927.0118. (Reprinted in Bull. Math. Biol., 53 (1991), pp. 33–55.)
[23] R.-M. Lana, T.G.S. Carneiro, N.A. Honório, and C.T. Codeço, *Seasonal and nonseasonal dynamics of Aedes aegypti in Rio de Janeiro, Brazil: Fitting mathematical models to trap data*, Acta Tropica, 129 (2014), pp. 25–32. doi:10.1016/j.actatropica.2013.07.025.
[24] J. Medlock, P.M. Luz, C.J. Struchiner, and A.P. Galvani, *The impact of transgenic mosquitoes on dengue virulence to human and mosquitoes*, American Naturalist, 174 (2009), pp. 565–577. doi:10.1086/605403.
[25] H. Minc, *Nonnegative Matrices*, Wiley-Interscience, New York, 1988.
[26] D. Mollison, *The rate of spatial propagation of simple epidemics*, in Proceedings of the Sixth Berkeley Symposium on Mathematical Statistics and Probability, Vol. 3, University of California Press, Oakland, CA, 1972, pp. 579–614.
[27] J.D. Murray *Mathematical Biology:* I. *An Introduction*, 3rd ed., Springer-Verlag, New York, 2002.
[28] J.D. Murray, *Mathematical Biology*, Springer, Berlin, 1989.
[29] Secretaria de Estado de Transporte, Governo do Estado do Rio de Janeiro, *Plano Diretor de Transporte Urbano da Região Metropolitana do Rio de Janeiro*, Technical report, 2014. Available online at http://www.seaerj.org.br/pdf/PDTUSEAERJ.pdf.
[30] Secretaria Municipal de Saúde–SMS, *Casos de Dengue por Bairro e Período (Infected Cases of Dengue per Neighborhood and Period)*, Prefeitura do Rio de Janeiro, Cidade Nova, Rio de Janeiro, Brazil, 2015. http://www.rio.rj.gov.br/web/sms/exibeconteudo?id=2815389.
[31] C.P. Simmons, J.J. Farrar, N.V. Chau, and B. Wills, *Dengue*, New Engl. J. Med., 366 (2012), pp. 1423–1432. doi:10.1056/NEJMra1110265.
[32] L.M. Stolerman, *The Spreading of an Epidemic over a City: A Model on Networks*, Master's Thesis, Universidade Federal de Rio de Janeiro, Rio de Janeiro, Brazil, 2012 (in Portuguese).
[33] Superintenência de Vigilância Epidemiológica e Ambiental do Estado do Rio de Janeiro, *Boletim Epidemiológico e Ambiental*, 2009/2010. Available online at http://www.saude.rj.gov.br/vigilancia-em-saude/791-vigilancia-epidemiologica/6482-boletim-epidemiologicoe-ambiental-2009-2010.html.
[34] M.G. Teixeira, M.C. Costa, F. Barreto, and M.L. Barreto, *Dengue: Twenty-five years since reemergence in Brazil*, Cad. Saúde Pública, 25 (Suppl.) (2007), pp. S1–S18. doi:10.1590/S0102-311X2009001300002.

[35] A. Troyo Guerrero, *Modelo SIR em Rede e com Parâmetro de Infeção Que Depende Periódicamente do Tempo*, Master's thesis, COPPE/UFRJ - Instituto Alberto Luiz Coimbra de Pós-Graduação e Pesquisa de Engenharia, Rio de Janeiro, Brazil, 2013.
[36] H. Weiss, *A Mathematical Introduction to Population Dynamics*, Instituto Nacional de Matemática Pura e Aplicada (IMPA), Rio de Janeiro, Brazil, 2009.
[37] World Health Organization (WHO), *Dengue and Severe Dengue*, Fact sheet 117, 2015. http://www.who.int/mediacentre/factsheets/fs117/en.